A novel interaction between the 5' untranslated region of the Chikungunya virus genome and Musashi RNA binding protein is essential for efficient virus genome replication

Authors: Kaiwen Sun, Marietta Müller, Catriona Macfarlane, Mark Harris and Andrew Tuplin*

Correspondence: a.k.tuplin@leeds.ac.uk

Affiliations: Astbury Centre for Structural Molecular Biology and School of Molecular and Cellular Biology, Faculty of Biological Sciences, University of Leeds, Leeds LS2 9JT, UK.

Abstract

Chikungunya virus (CHIKV) is a re-emerging, pathogenic alphavirus that is transmitted to humans by *Aedes spp*. mosquitoes—causing fever and debilitating joint pain, with frequent long-term health implications and high morbidity. The CHIKV lifecycle is poorly understood and specific antiviral therapeutics or vaccines are lacking. In the current study, we identify host cell Musashi RNA binding protein-2 (MSI-2) as a proviral factor. MSI-2 depletion and small molecule inhibition assays, demonstrated that MSI-2 is required for efficient CHIKV genome. Depletion of both MSI-2 and MSI-1 homologues resulted in a synergistic increase in CHIKV inhibition, suggesting redundancy in their proviral function. EMSA competition studies demonstrated that MSI-2 interacts specifically with an RNA binding motif within the 5' untranslated region (5'UTR) of CHIKV and reverse genetic analysis showed that mutation of the binding motif inhibited genome replication and blocked rescue of mutant virus. For the first time, this study identifies the proviral role of MSI RNA binding proteins in the replication of the CHIKV genome, providing important new insight into mechanisms controlling replication of this significant human pathogen and offers the potential of a new therapeutic target.

INTRODUCTION

46 Chikungunya virus (CHIKV) is an alphavirus of the *Togaviridae* family that is
47 transmitted by *Aedes spp.* mosquitos. CHIKV is closely related to other alphaviruses
48 such as Semliki Forest virus (SFV), Venezuelan equine encephalitis virus (VEEV), and
49 sindbis virus (SINV) [1, 2]. CHIKV was first identified in Tanzania in 1952 and
50 symptoms typically include acute febrile symptoms, myalgia, rash and severe
51 arthralgic joint pain, which may persist for months or years [3]. CHIKV recently
52 caused epidemic outbreaks across regions in Asia, Africa, the Americas, the Middle
53 East and Southern Europe [3]. To date, three phylogenetically distinct lineages of
54 CHIKV have been identified, namely the West African, Asian and the East Central
55 Southern African (ECSA) lineages [4]. There remains no clinically approved vaccine or
56 specific antiviral therapy, due in part to a lack of detailed understanding of the CHIKV
57 replication cycle and its interaction with host cell factors.
58
59 CHIKV is an enveloped, positive-sense single-stranded RNA virus with a ~11.8 Kb
60 genome, containing two open reading frames (ORFs) flanked by 5' and 3'
61 untranslated regions (UTRs) (**Fig. 1A**). The 5' UTR is ~ 76 nts in length and is capped
62 by 5' type-0 N-7-methylguanosine. The upstream ORF (ORF-1) encodes the viral non-
63 structural proteins 1-4 (nsP1-4), which are translated directly from the genomic RNA
64 as a single polyprotein that is subsequently proteolytically cleaved into the four
65 mature proteins [5]. Through analogy with other alphaviruses, proteolytic cleavage
66 of nsP1-4 in *cis* by nsP2 releases nsP4 which, as the RNA-dependent RNA polymerase
67 (RdRp), initiates synthesis of the minus-strand intermediate RNA. Subsequent
68 proteolytic cleavage of the remaining nsP123 polyprotein initiates replication of
69 genomic and sub-genomic (29S) RNAs from the minus-strand template [6]. The

70 downstream ORF (ORF-2) encodes the structural polyprotein that is processed into
71 the capsid protein, E3, E2, 6K, and E1.
72
73 While negative strand replication is initiated at the 3' end of the virus genome, as
74 with many positive single stranded RNA viruses, regulatory elements and
75 interactions within the 5' end of the CHIKV genome are required for its initiation and
76 regulation [7]. We and others have previously demonstrated that such regulatory
77 elements include functional RNA secondary structures and higher order interactions
78 within the CHIKV 5'UTR and adjacent upstream region of ORF-1 (**Fig. 1B**). It has been
79 speculated that these RNA elements may regulate template specificity and temporal
80 control of switching, between CHIKV translation and genome replication [8, 9].
81
82 In a previously published study, we demonstrated by SHAPE mapping and reverse
83 genetic analysis that the CHIKV 5'UTR and adjacent ORF-1 coding region is highly
84 structured [9]. However, the study also highlighted a single-stranded region (nts 63-
85 69) that exhibited very high SHAPE reactivity (associated with unpaired bases) and
86 was located immediately between two RNA structures, that we demonstrated were
87 essential for initiation of CHIKV genome replication **(Fig 1B)**. Interestingly, *in silico*
88 analysis noted that nts ^{63}AUUAAU^{68} were closely homologous to the Musashi RNA
89 binding protein (MSI) consensus binding sequence ((G/A)U_{1-3}AGU). MSI are highly
90 conserved RNA binding proteins, containing two highly conserved tandem RNA
91 recognition motifs (RNP-1 and RNP-2), that interact with RNA via the same
92 consensus binding motif. Two MSI homologues have been identified, MSI-1 and MSI-
93 2, that share over 90% homology in their RNA-binding domains and a high degree of

94 functional complementarity and redundancy [10, 11]. MSI have key roles in post-
95 transcriptional regulation of genes involved in development, cell cycle regulation and
96 maintenance of adult neural stem/progenitor cells [12]. A recent study
97 demonstrated that MSI-1 promotes Zika Virus (ZIKV) genome replication in neurons,
98 via interaction with the consensus binding site within the viral 3'UTR [13].
99
100 In the current study, we demonstrate through a range of infectious clone and sub-
101 genomic replicon reporter assays that MSI-2 is required for efficient CHIKV genome
102 replication. A small molecule inhibitor of MSI-1 and MSI-2 reduced infectious virus
103 production by inhibition of CHIKV genome replication. Similarly, MSI-2 silencing by
104 shRNA and siRNA inhibited both infectious virus production and genome replication,
105 while co-silencing of both MSI-2 and MSI-1 resulted in a synergistic increase in
106 inhibition of CHIKV replication. Reverse genetic analysis, in which the putative MSI
107 binding site within the CHIKV 5'UTR was mutated, completely prevented rescue of
108 mutant virus and inhibited CHIKV genome replication. Biochemical MSI-2 binding
109 analysis by competition electromobility shift assay (EMSA) demonstrated that
110 recombinantly expressed MSI-2 specifically interacts with the 5' region of the CHIKV
111 genome and that this interaction is inhibited by mutation of the putative MSI 5'UTR
112 binding site. These findings demonstrate for the first time that interaction between
113 MSI and a binding site within the 5'UTR are required for replication of the CHIKV
114 genome.
115
116 **Materials and Methods**
117

118 **Cell culture**

119 Human Rhabdomyosarcoma (RD), Human hepatoma (Huh7), Baby Hamster Kidney
120 (BHK) and Human Embryonic Kidney (HEK) 293 were grown in Dulbecco's modified
121 eagle's medium (DMEM; Sigma) containing 10% fetal bovine serum (FBS; PAA), 1x
122 penicillin-streptomycin (Sigma), 25mM HEPES in 0.85% NaCl (Lonza) and 1% non-
123 essential amino acids mixture (NEAA; Lonza). Cells were harvested using
124 trypsin/EDTA, seeded at dilutions of 1:3 to 1:10 and maintained at 37°C in 5% CO_2.

125

126 **CHIKV cDNA plasmid**

127 The infectious CHIKV (ICRES), CHIKV Dual-luciferase sub-genomic replicon (CHIKV-
128 SGR) and *trans*-complementation (pCHIKV-nsP1234 and pCHIK-Fluc/Gluc) assay were
129 derived from the CHIKV ESCA strain, isolate LR2006 OPY1 (accession number
130 DQ443544)[14]. In CHIKV-SGR the second ORF was replaced by a firefly luciferase
131 gene and a *Renilla* luciferase gene was fused within nsP3 [15]. The *trans*-
132 complementation assay utilised a CMV codon optimised plasmid to supply the CHIKV
133 replicase in *trans* (pCHIKV-nsP1234) and a Pol II expressed reporter plasmid (pCHIKV-
134 FLuc/GLuc), in which the majority of ORF-1 (downstream of nt 320) was replaced by
135 a firefly luciferase gene and all of ORF-2 by a Gaussia Luciferase gene [16]. Plasmid
136 cDNA was purified using GeneJET Plasmid Maxiprep kits (Thermo Fisher Scientific)
137 according to the manufacturer's instructions.

138 **Virus production**

139 1×10^6 BHK cells were trypsinised and resuspended in 400 µl ice-cold DEPC-PBS. Cells
140 were then electroporated with 1 µg 5'-capped CHIKV ICRES *in vitro* transcribed RNA

141 in a 4 mm electro-cuvette, with a single square wave pulse at 260 V for 25 ms using a
142 Bio-Rad electroporator, before seeding into a T175 flask in 20 ml DMEM. After 24 h,
143 supernatant was aspirated and virus titre measured by plaque assay on BHK cells.
144

145 **CHIKV quantification by plaque assay**

146 BHK cells were seeded at 1×10^5 cells per well in 12-well plates and maintained
147 overnight in 1 ml DMEM. The following day monolayers were washed with PBS,
148 infected with 10-fold serial dilutions of CHIKV transfection supernatant and
149 maintained at 37 °C. 1 hpi monolayers were washed with PBS and covered with a
150 0.8% methylcellulose DMEM P/S overlay. 48 hpi monolayers were fixed and stained
151 (5% paraformaldehyde and 0.25% crystal violet respectively), plaques counted and
152 virus titres expressed in plaque-forming units per ml (PFU/ml).
153

154 **Ro 08-2750 cell viability assay**

155 RD cells were seeded in 96-well plate at $8x10^4$ cells/well and maintained for 24 hrs.
156 Monolayers were then treated with increasing doses (0, 0.5, 1, 3, 5, 7, 10, 20 µM) of
157 Ro 08-2750 (TOCRIS) dissolved in DMSO. After 24 hrs media/inhibitor was aspirated
158 and replaced with 20 µl of 5 mg/mL 3-(4,5-dimethylthiazol-2-yl)-2,5-
159 diphenyltetrazolium bromide (MTT) (Sigma) and incubated at 37 °C in 5% CO_2 for 3
160 hrs. After incubation, MTT solution was replaced with 100 µl DMSO and the plate
161 shaken at 60 rpm for 5 min. Absorbance at 570 nm was determined using an Infinite
162 F50 microplate reader (Tecan) and expressed as a percentage of DMSO control cells.

163 5 µM Ro 08-2750 was estimated to be the maximum non-toxic dose in in Huh7 cells
164 and was used for all further assays.
165
166 **Infectious CHIKV Ro 08-2750 inhibition assays**
167 RD cells were seeded in 12-well plates at $1x10^5$ cells/well and incubated overnight in
168 the presence of Ro 08-2750. Monolayers were then infected with CHIKV at MOI=0.1
169 and adsorbed to the cells for 1 h at 37°C before aspirating and maintaining in the
170 presence of Ro 08-2750 for 24 hrs. Supernatants was then collected and infectious
171 virus production measured by plaque assay.
172
173 **siRNA depletion of MSI-1 and MSi-2**
174 RD or Huh7 cells were seeded at $1x10^5$ cell/well in 12-well plates in antibiotic-free
175 medium. After 24 hrs, cells were washed with PBS and incubated with 1x Opti-MEM
176 + GlutaMAX (Gibco) for 20 min at 37°C/5% CO_2. For each well, 50 pmol MSI-1 (sc-
177 106836; Santa Cruz) and/or MSI-2 siRNA (sc-75834; Santa Cruz) were mixed with 100
178 µl Opti-MEM and incubated at room temperature for 1min. No siRNAs were added
179 to mock samples and 50 pmol of scrambled siRNA (SI03650318; QIAGEN) was used
180 as a negative control. In parallel, 3 µl Lipofectamine RNAiMAX (Invitrogen) was
181 mixed with 100 µl Opti-MEM and incubated at room temperature for 1 min. The
182 siRNA and Lipofectamine RNAiMAX were mixed and incubated at room temperature
183 for 5 min before adding to the cells. After 24 hrs, cells were either lysed to confirm
184 MSI-1 or MSi-2 depletion by western blot or used for subsequent CHIKV infection
185 assays.
186

187 **shRNA depletion of MSI-1 and MSi-2**

188 Human embryonic kidney 293 (HEK 293T) cells were plated in antibiotic-free DMEM
189 in 6-well plates and maintained until confluency reached ~80%. For each
190 transfection, in a single tube 300 µL OptiMEM was mixed with 1 µg p8.9 packaging
191 plasmids, 1 µg envelope plasmid and either 1.5 µg MSI-2 shRNA or scrambled shRNA
192 (Santa Cruz Biotechnology); in another tube, 300 µL of OptiMEM was mixed with 5
193 µL lipofectamine 2000 (Invitrogen). Both tubes were gently mixed by flicking,
194 incubated at room temperature for 5 min, mixed together and incubated for 20 min
195 at room temperature. The antibiotic-free DMEM was aspirated and the monolayers
196 washed once with PBS. 800 µL Opti-MEM was added to each well before dropwise
197 addition of the lentiviral plasmids/shRNA mixture. After maintenance at 37°C for 6
198 hrs the media was changed to antibiotic-free DMEM. 48 hpt the lentivirus containing
199 supernatant was harvested and filtered through a 0.45 µm filter.

200

201 RD cells were seeded at $1x10^5$ cells/well the day prior to transduction. 1 mL of the
202 lentivirus supernatant and polybrene (MERCK) were added to each well and
203 incubated for 6 hrs before aspirating and replacing with antibiotic free DMEM. After
204 72 hrs media was replaced with DMEM containing 2.5 µg/ml puromycin, in which the
205 cells were then maintained. The efficiency of the shRNA MSI-2 depletion was
206 confirmed by western blot.

207

208 **Strand-specific Quantification of CHIKV RNA**

209 Total RNA was extracted from infected cells using TRI Reagent Solution (Applied
210 Biosystems) according to the manufacturer's instructions. Strand-specific RT-qPCR
211 (ssRT-qPCR) was performed as previously described [17]. Briefly, 500 ng of RNA was
212 reverse-transcribed with gene specific primers (Supplementary information 1) using
213 the SCRIPT cDNA Synthesis Kit (Jena Bioscience) according to the manufacturer's
214 protocol. 100 ng of strand-specific cDNA was used as template for the quantitative
215 PCR performed with the qPCRBIO SyGreen Blue Mix Lo-ROX (PCR Biosystems), with
216 gene specific primers amplifying a 94 bp region of the CHIKV nsP1-encoding
217 sequence using the following PCR program: 95°C for 2 mins, 40 x (95°C for 5 sec,
218 60°C for 30 sec), dissociation curve 60°C-95°C as pre-defined by the Mx3005P
219 thermal cycler (Agilent technologies). *In vitro* transcribed CHIKV ICRES RNA was
220 reverse transcribed and a cDNA dilution series employed as a standard to quantify
221 copy numbers in the respective samples.

222

223 ***In vitro* RNA transcription**

224 To generate CHIKV-SGR and infectious CHIKV RNA, 2 µg of cDNA was linearised with
225 Not-I HF and used as a template for transcription of 5' [m7G(5')ppp(5')G] capped
226 (m7G capped) RNA, using an SP6 mMessage mMachine kit, according to the
227 manufacturer's instructions (Life Technologies). Uncapped CHIKV 1–337 RNA, used
228 1 µg of CHIKV 1–337 PCR DNA as a template for *in vitro* transcription using the SP6-
229 Scribe™ standard RNA IVT kit, according to the manufacturer's instructions (Lucigen).

230 In all cases, following DNase I treatment, RNA was purified by LiCl precipitation and
231 analysed by denaturing agarose gel electrophoresis.
232

233 **CHIKV Sub-genomic replicon assays**

234 For analysis of Ro 08-2750 inhibition, RD cells were seeded in 24 well plates at
235 5×10^4 cells per well and maintained overnight in the presence of Ro 08-2750.
236 Monolayers were washed once in PBS before addition of 400 µl opti-Mem reduced-
237 serum media and 100 µl transfection media. Transfection media was prepared
238 according to the manufacturer's instructions, using 1 µl Lipofectamine 2000
239 (Invitrogen), 250 ng of CHIKV-SGR RNA and appropriate concentrations of Ro 08-
240 2750, before being made up to 100 µl using opti-Mem. Monolayers were maintained
241 for 6 hpt before the media was aspirated and replaced with complete DMEM/Ro 08-
242 2750. At 8 and 24 hpt monolayers were lysed with 100 µl 1 x passive lysis buffer
243 according to the manufacturer's instructions (Promega), stored at −80 °C and
244 analysed using Dual-luciferase substrate (Promega) in a FLUOstar Optima
245 luminometer (BMG labTech). For shRNA MSI-2 depleted cell lines the same method
246 was followed, with the exclusion of Ro 08-2750.
247

248 ***Trans*-complementation Assay**

249 The *trans*-complementation assay was performed as previously described [18].
250 Briefly, for analysis of Ro 08-2750 inhibition, RD cells were seeded in 12 well plates at
251 5×10^4 cells per well and maintained overnight in the presence of Ro 08-2750.
252 Monolayers were then co-transfected with 1 µg each of the pCHIKV-nsP1234 and

253 pCHIKV-FLuc/GLuc using Lipofectamine 2000, as described previously, and assayed
254 at 8 and 24 hpt. For shRNA MSI-2 depleted cell lines the same method was followed,
255 with the exclusion of Ro 08-2750.
256
257 **Expression and purification of recombinant MSI-2 RNA binding domains**
258 The MSI-2 RNA binding domain expressing plasmid pET-22HT-MSI-2 (amino acid 8-
259 193) was a kind gift from Prof S. Ryder (Addgene plasmid # 60356;
260 http://n2t.net/addgene:60356; RRID: Addgene_60356) [19]. The plasmid was
261 transformed into BL21 (DE3) competent cells following the manufacturer's protocol
262 (NEB), a single colony was inoculated into 10 mL LB ampicillin (10 mg/ml) and
263 incubated overnight at 37°C before inoculating 1000 ml 1 LB (ampicillin (10 mg/ml)
264 and adding 100 µM Isopropyl β-D-1-thiogalactopyranoside (IPTG; Thermo Fisher
265 Scientific) when the optical density reached 0.8. The culture was then incubated
266 overnight at 18°C in an orbital shaker before centrifugation to pellet the bacteria.
267 The pellet was resuspended in lysis buffer (20U/mL DNase I, 0.6U/mL RNase A,
268 1mg/mL lysozyme and 1x protease inhibitor) and lysed on ice for 30 min . Following
269 sonication, the suspension was centrifuged twice at 2000 xg for 1 hour at 4°C. The
270 was filtered through a 0.45 µm filter and His-MSI-2 was purified with HisTrap^{TM} FF
271 column (Cytiva) using the Econo Gradient Pump (BIORAD) according to the
272 manufacturer's protocol and overnight dialysis. The purified protein was quantified
273 and the purity and identity assayed by Coomassie SDS-PAGE and western blot
274 (Supplementary data 2).
275

276 After desalting using PD-10 desalting columns (Cytiva), His-MSI-2 protein was further
277 purified by ion exchange chromatography. Following the manufacturer's
278 instructions, the column was equilibrated with wash buffer (50 mM MES, 10 mM
279 NaCl, pH 5.6, degassed) and the protein eluted in the same buffer. Ion exchange
280 chromatography was performed using HiTrap SP HP cation exchange
281 chromatography column (Cytiva) following the manufacturer's instructions and
282 eluted in degassed 50mM MES, 1M NaCl, pH 5.6. The eluted protein fractions were
283 analysed by Coomassie SDS-PAGE and western blot (Supplementary data 2).
284
285 **^{32}P RNA end labelling**
286 *In vitro* transcribed CHIKV RNA (nt's 1-337) was 5' dephosphorylated using Quick CIP
287 according to the manufacturer's instructions (NEB) before purification using an RNA
288 Clean & Concentrator column (Zymo Research). 20 pmoles of dephosphorylated RNA
289 was combined with 2 µl 10 x T4 Polynucleotide Kinase buffer (NEB), 3 µl ATP(γ-^{32}P)
290 10 mCi/ml, 1 µl T4 Polynucleotide Kinase (NEB) and nuclease free H_2O to a final
291 volume of 20 µl, incubated at 37 °C for 60 min, 65 °C for 20 min, purified using an
292 RNA Clean & Concentrator Kit (Zymo Research) and resuspended in RNase-free H_2O.
293
294 **Electromobility shift assay (EMSA)**
295 RNA was incubated at 95°C for 2 min and on ice for 2 min before 3.3 x RNA folding
296 buffer (100 mM HEPES pH 8.0, 100 mM NaCl and 10 mM MgCl2) and RNasin Plus
297 RNase Inhibitor (Promega) was added to a final volume of 10 µl and incubated for
298 20 min at 37°C. MSI-2 protein was combined with 3.3 x RNA folding buffer, 0.5 x TE,
299 100% glycerol, RNasin Plus RNase Inhibitor (Promega) and 5 µg yeast tRNA as non-

300 specific competitor and incubated at 37°C for 2 min before adding to the RNA
301 mixture and further incubation at 37°C for 15 min. Finally, samples were analysed by
302 native PAGE gel electrophoresis at 135 V for ~2 h. The gel was fixed for 30 min and
303 dried with gel dryer (BIORAD), exposed onto Hyperfilm™ ECL™ (Merck) and
304 visualised using a Xograph Film Processor. Band shifts were quantified by
305 densitometry, as a percentage of band density normalised to the total lane density,
306 relative to control lanes.
307

308 **Assessment of MSI-1, MSI-2 and CHIKV protein expression by western blot**

309 Following infection and incubation, monolayers were lysed in IP lysis buffer
310 (Promega) and incubated at room temperature for 30 min. Protein concentration
311 was quantified using a Pierce™ BCA Protein Assay Kit (Thermo scientific) according to
312 the manufacturer's instructions. Equal amounts of protein lysate were analysed by
313 SDS-PAGE. Protein was transferred onto an Immobilon-FL PVFD transfer membrane
314 (MERCK) using a TE77X semi-dry transfer (Hoefer) at 15 V for 60 min. Membranes
315 were blocked using diluted Odyssey® Blocking Buffer in PBS (LI-COR) for 30 min and
316 probed with primary antibodies against β-actin (1:10,000, mouse monoclonal, Sigma-
317 Aldrich A1978), MSI-2 (1:1000 rabbit monoclonal, Abcam ab76148) and MSI-1
318 (1:5000, Abcam ab21628) in diluted Odyssey® Blocking Buffer in PBS (LI-COR)
319 overnight at 4 °C. After overnight incubation, primary antibody was removed and
320 membranes washed 3 times using PBS. Membranes were stained with secondary
321 antibodies (IRDye® 800CW Donkey anti-Mouse; IRDye® 680LT Donkey anti-Rabbit; Li-

322 Cor) for 1 h at room temperature, washed 3 times using 1 x PBS, dried and then
323 imaged using an Odyssey® Fc Imaging System (Li-Cor).
324
325 ***Statistical analysis***
326 Statistical analysis was carried out using one-way ANOVA and Dunnett's multiple
327 comparisons test on GraphPad Prism version 8.4.0. *P* values of ≤0.05 (*), ≤0.01 (**),
328 ≤0.001 (***) were used to represent degrees of significance between each drug
329 treatment/silencing/mutant to wild-type assay.
330
331 **RESULTS**
332
333 **Ro inhibited replication of CHIKV infectious virus and sub-genomic replicon:**
334 In order to investigate the potential role of MSI on CHIKV replication, we first
335 assessed the effect of a well-characterised MSI small molecule inhibitor, Ro 08-2750
336 (Ro), on CHIKV productive replication in RD cells using both CHIKV infectious virus
337 and a sub-genomic replicon (SGR) assay (Fig 2A). A number of studies have
338 demonstrated that Ro interacts with the MSI RNA binding domains and acts as a
339 competitive inhibitor for its RNA binding activity and subsequent MSI functions
340 within the cell [20, 21] [22]. In the current study Ro was used at a maximum non-
341 toxic dose as determined by MTT assay (Supplementary data 3).
342
343 The effect of Ro on productive CHIKV infection was measured at 8 and 24 hpi and it
344 was observed that pre-treatment and incubation in the presence Ro significantly

345 inhibited infectious CHIKV replication by ~10-fold, relative to DMSO treated negative
346 controls (Fig. 2B). In order to investigate the effect of Ro on specific stages of CHIKV
347 replication we used an SGR construct, in which ORF-2 was replaced by a firefly
348 luciferase (FLuc) gene and a *Renilla* luciferase (Rluc) gene was fused in-frame with
349 ORF-1 nsP3 (Fig 2A)[9]. The SGR assay enabled us to measure the effect of Ro on
350 CHIKV genome replication and translation, in isolation of other stages of virus
351 infection, such as entry or egress. SGR ORF-1 and ORF-2 expression was significantly
352 inhibited at both 8 and 24 hpt, relative to DMSO treated negative controls, indicating
353 that Ro was inhibiting CHIKV replication at the level of virus genome replication or
354 translation (Fig 2C). ORF-1 is translated from full-length genomic transcripts and ORF-
355 2 from 18S sub-genomic transcripts. The observed inhibition of both ORF-1 and ORF-
356 2 expression was consistent with Ro acting at a stage of the replication cycle common
357 to expression of both ORFs.
358
359 **Ro inhibited CHIKV *trans*-complementation assay:**
360 Inhibition of SGR replication demonstrated that Ro was inhibiting CHIKV replication
361 at the level of virus genome replication or translation. In order to dissect this further,
362 we utilised a *trans*-complementation assay, that enabled the measurement of CHIKV
363 genome replication in isolation of virus translation (Fig 3A)[23]. The *trans*-
364 complementation system utilised a codon-optimised CHIKV replicase-expressing
365 plasmid (pCHIKV-nsP1234), which expresses the virus nsPs from a CMV promoter.
366 The expressed nsPs replicate a CHIKV reporter construct (pCHIKV-FLuc/GLuc), in
367 which the majority of ORF-1 is replaced by an FLuc gene and ORF-2 by the Gaussia
368 luciferase (GLuc) gene. The effect of Ro on pCHIKV-FLuc/GLuc expression was

369 measured at 8 and 24 hpt in cells pre-treated with and maintained in the presence of
370 Ro. Both ORF-1 and ORF-2 expression was observed to be significantly inhibited
371 relative to the DMSO treated negative controls, indicating that Ro was inhibiting
372 CHIKV replication specifically at the level of virus genome replication.
373
374 **MSI-2 shRNA silencing inhibits infectious CHIKV replication:**
375 In order to confirm that Ro induced inhibition of CHIKV genome replication was due
376 to specific inhibition of MSI, rather than an unrecognised off target effect of Ro, we
377 next investigated CHIKV replication following shRNA silencing of MSI expression.
378 Analysis of RD cell total protein extract by western blot, demonstrated that MSI-2
379 was strongly expressed in RD cells while MSI-1 was expressed at a very low level
380 (Supplementary data 4). Consequently, we initially investigated the effect of specific
381 MSI-2 shRNA silencing on CHIKV replication. RD cells were transduced with lentiviral
382 vectors encoding shRNA against human MSI-2 and successful silencing was
383 confirmed by western blot (Fig 4A). Negative control cells were treated with either
384 transfection reagent only (mock) or non-specific scrambled shRNA. Following
385 infection of MSI-2 depleted and negative control cells, productive CHIKV infection
386 was measured by plaque assay at 8 and 24 hpi (Fig 4B). Strand specific qRT-PCR was
387 also used to measure levels of genomic (positive strand) and replication
388 intermediate (negative strand) CHIKV RNA at both time points (Fig 4 C and D). As
389 observed previously following treatment with Ro, relative to the scrambled shRNA
390 control productive CHIKV replication was significantly inhibited following shRNA MSI-
391 2 silencing (Fig 4B). Similarly, strand specific qRT-PCR demonstrated that both
392 genomic and replication intermediate CHIKV RNA levels were significantly inhibited

393 (Fig 4 C and D). These results are consistent with CHIKV requiring MSI-2 for efficient
394 genome replication.
395
396 **MSI-2 is required for efficient CHIKV genome replication**
397 In order to confirm that MSI-2 silencing had the same effect on CHIKV genome
398 replication as Ro small molecule inhibition, we repeated analysis with the SGR and
399 *trans*-complementation systems, following shRNA silencing of MSI-2. As previously
400 described, MSI-2 shRNA silenced RD cells were transfected with the SGR system and
401 ORF-1 and ORF-2 expression measured by RLuc and FLuc expression at 8 and 24 hpt
402 (Fig 5A and B). Expression of both ORF-1 and ORF-2 was significantly inhibited at
403 both 8 and 24 hpt, consistent with an MSI-2 requirement for CHIKV genome
404 replication or translation. Analysis at the same time points using the *trans*-
405 complementation system, following shRNA MSI-2 silencing and measuring ORF1 and
406 ORF2 expression, confirmed significant inhibition of CHIKV genome replication when
407 measured in isolation of the effects of other stages of the virus replication cycle (Fig
408 5C and D)
409
410 **Both MSI-2 and MSI-1 have a proviral effect on CHIKV genome replication:**
411 While results clearly demonstrated that MSI-2 was required for efficient CHIKV
412 replication, it remained unclear if MSI homologue MSI-1 was also agonistic for CHIKV
413 replication. As previously described, western blot analysis showed that MSI-1 was
414 not highly expressed in RD cells. Consequently, we analysed MSI homologue
415 redundancy in Huh7 human hepatoma cells, in which both MSI-1 and MSI-2
416 homologues are strongly expressed (Supplementary data 4) and are highly

417 permissive for CHIKV replication [24]. Following individual and combined siRNA
418 silencing of MSI-1 and MSI-2 in Huh7 cells (Supplementary data 5), CHIKV replication
419 was assayed by plaque assay and ssRT-qPCR at 8 and 24 hpi (Fig 6A, B and C). As was
420 observed for RD cells, MSI-2 silencing significantly inhibited CHIKV replication,
421 measured by both plaque assay and strand specific ssRT-qPCR. Interestingly, it was
422 observed that MSI-1 silencing in Huh7 cells had a similar significant inhibitory effect
423 and that siRNA co-silencing of both MSI-1 and MSI-2 had a synergistic effect on
424 inhibition of CHIKV replication. In concordance with previous results, siRNA silencing
425 of MSI-2 in RD cells significantly inhibited CHIKV replication, by comparable levels
426 observed following shRNA silencing and inhibition by Ro. Consistent with low MSI-1
427 expression in RD cells, siRNA co-silencing of both MSI-1 and MSI-2 did not
428 significantly increase levels of CHIKV inhibition (Fig. 6D, E and F).
429
430 **MSI-2 binds specifically to the predicted $_{63}$AUUAAU$_{68}$ 5'UTR MSI binding site in the**
431 **CHIKV 5'UTR**
432 Following confirmation that MSI-2 RNA binding protein is required for efficient CHIKV
433 genome replication, we next used native EMSA to biochemically investigate the
434 potential for a direct interaction between the RNA binding domains of MSI-2 and
435 nucleotides $_{63}$AUUAAU$_{68}$ within the virus 5'UTR, which had close sequence homology
436 to the (G/A)U$_{1-3}$AGU MSI consensus nucleotide binding motif [25]. $_{63}$AUUAAU$_{68}$ is
437 located in single-stranded region of the 5' UTR, 9 nts upstream of the AUG start
438 codon and between two RNA structures that are essential for CHIKV genome
439 replication (Fig. 1B)[9]. The first 330nts of the CHIKV genome (RNA-330),
440 representing the 5'UTR and adjacent upstream region of ORF1, was *in vitro*

441 transcribed, 5' end radiolabelled with ATP-[γ-32P] and incubated at 37°C - conditions
442 under which correct folding of the functional RNA-330 structure was previously
443 validated [9]. Following incubation with increasing concentrations of recombinantly
444 expressed and purified MSI-2 8-193 in the presence of unlabelled tRNA, reaction
445 products were separated by native PAGE and analysed by autoradiography (Fig 7A).
446 Relative to unbound RNA-330, the presence of MSI-2 8-193 resulted in the
447 retardation of RNA-330 migration during native PAGE, consistent with the formation
448 of an RNA-330/MSI-2 8-193 complex. In order to investigate the specificity of the
449 observed interaction, a fixed molar ratio of RNA-330$^{\gamma\text{-}32P}$ and MSI-2 8-193 was
450 incubated with increasing concentrations of competitor unlabelled RNA-330 (Fig 7B).
451 Increasing concentrations of unlabelled RNA-330 reduced the formation of the RNA-
452 330$^{\gamma\text{-}32P}$/MSI-2 8-193 complex, with a corresponding increase in unbound RNA-330$^{\gamma\text{-}}$
453 ^{32P}.
454
455 In order to further confirm the specificity and location of the interaction the putative
456 MSI-2 binding site $_{63}$AUUAAU$_{68}$ was mutated to $_{63}$CAACUU$_{68}$ (henceforth termed
457 $_{63}$CAACUU$_{68}$-mut). EMSA competition with unlabelled $_{63}$CAACUU$_{68}$-mut RNA-330 was
458 significantly less efficient at competing for MSI-2 8-193 binding than wild-type CHIKV
459 RNA (Fig 7 C and D). These ESMA results are consistent with an interaction between
460 MSI-2 and the upstream region of the CHIKV genome. The significant inhibition of
461 this interaction in the $_{63}$CAACUU$_{68}$-mut indicated both that the interaction was
462 specific and that nts $_{63}$AUUAAU$_{68}$ function as an MSI binding motif.
463

464 **Mutagenesis of 5'UTR $_{63}$AUUAAU$_{68}$ MSI binding site inhibits CHIKV genome**
465 **replication and prevents virus rescue**
466 In order to further investigate the role of the $_{63}$AUUAAU$_{68}$ MSI binding motif in CHIKV
467 replication, we took a reverse genetic approach, in which the
468 $_{63}$AUUAAU$_{68}$>$_{63}$CAACUU$_{68}$ mutations were incorporated into both the *trans*-
469 complementation assay and infectious CHIKV. Similar to previous results following
470 MSI inhibition, expression of both ORF-1 and ORF-2 from the *trans*-complementation
471 system were significantly inhibited in $_{63}$CAACUU$_{68}$-mut relative to the wild type at 8
472 and 24 hpt (Fig 8A and B); indicating that mutation of the putative MSI binding site
473 significantly inhibited CHIKV at the level of virus genome replication. Interestingly,
474 despite repeated attempts, we were not able to rescue infectious CHIKV $_{63}$CAACUU$_{68}$-
475 mut virus, indicating that disruption of the potential MSI binding site completely
476 inhibited infectious CHIKV replication (Fig 8C).
477
478 **DISCUSSION**
479
480 For the first time, in this study we demonstrate that cellular RNA binding protein MSI
481 is required for efficient CHIKV replication. Our data demonstrates that MSI-2
482 interacts directly with the 5' end of the CHIKV genome and is consistent with an
483 interaction at position $_{63}$AUUAAU$_{68}$. A single-stranded region located between two
484 conserved stem-loops and immediately upstream of the AUG start codon (Fig 1) [9].
485 Inhibition of MSI-2 expression by siRNA or shRNA, its RNA-binding activity by Ro and
486 reverse genetic disruption of the CHIKV-5'UTR/MSI-2 interaction, inhibited CHIKV

487 replication at the level of virus genome replication. In further analysis, we
488 demonstrated that depletion of both MSI-1 and MSI-2 homologues resulted in a
489 synergistic increase in the level of CHIKV inhibition, supporting the premise that both
490 MSI homologues have a redundant pro-viral effect on CHIKV replication.
491
492 While depletion of MSI-2 by siRNA and shRNA clearly demonstrated significant
493 inhibition of CHIKV replication, measured by infectious virus production, CHIKV-SGR
494 replication or a *trans*-complementation assay, we did not observe complete
495 inhibition of virus replication. Western blot analysis indicated that we did not
496 achieve complete ablation of MSI-2 expression by either siRNA or shRNA,
497 presumably reducing the level of CHIKV inhibition observed. We demonstrated by
498 western blot that in RD cells MSI-2 is expressed to a high level but the MSI-1
499 homologue is only expressed to a low level. However, given the synergistic effect
500 that we observed when silencing expression of both MSI-2 and MSI-1 in Huh7 cells
501 (in which both are expressed to high levels), the ability of MSI homologues to
502 complement for each other may also have reduced the level of CHIKV inhibition
503 observed. This hypothesis is consistent with reverse genetic results, in which
504 mutation of the $_{63}$AUUAAU$_{68}$ MSI binding site, dramatically inhibited the CHIKV-
505 5'UTR/MSI-2 binding affinity and completely prevented rescue of mutant virus.
506
507 Translation and replication of positive-sense RNA virus genomes, such as those of
508 CHIKV are mutually exclusive processes – with translation initiating at the 5' end of
509 the genome and replication at the 3'. Consequently, it is essential that such viruses
510 have mechanisms for temporal control of both processes. In many such viruses (e.g.

511 Hepatitis C virus and Polio virus) control involves dynamic interactions between RNA
512 structures in the virus genome and host/virally expressed protein complexes [7]. The
513 mechanisms and interactions which CHIKV and other alphaviruses use for temporal
514 control of genome translation and replication remain unclear. However, a recent
515 study suggested a crucial role for the cellular helicase DHX9. Matkovic et al,
516 demonstrated that interaction between DHX9 and the 5' end of the virus genome
517 upregulates CHIKV ORF-1 non-structural protein translation, while simultaneously
518 inhibiting replication of its genome [26]. Build-up of nsP2 caused proteosome
519 induced degradation of DHX9, although the detailed mechanism for this remains
520 unclear.
521
522 While, genome replication of positive-sense RNA viruses initiates at the 3' end, it is
523 commonly controlled by promoter elements and interactions with RNA binding
524 proteins at the 5' end. Results described in this and previous studies are consistent
525 with a model in which temporal control of CHIKV ORF-1 translation and genome
526 replication is controlled by a mechanism involving interactions between DHX9, MSI2
527 and the 5' region of the virus genome. However, the dynamics and mechanism by
528 which the opposing roles if MSI-2 and DHX-9 influence CHIKV replication and their
529 interactions with the virus genome remains unclear and is the focus of ongoing
530 studies.
531
532 In summary, using MSI-2 depletion and Ro small molecule inhibitor we demonstrate
533 that MSI-2 RNA binding protein is a critical host factor for efficient CHIKV replication.
534 Inhibition of ORF-1 and ORF-2 signal from the *trans*-complementation assay indicate

535 that MSI-2 is required at the level of CHIKV genome replication. Furthermore, EMSA
536 and reverse genetic results are consistent with a direct interaction between MSI-2
537 and $_{63}$AUUAAU$_{68}$ in the positive genomic strand of the virus 5'UTR, suggesting a role
538 in negative strand synthesis. Results from this study are important both for our
539 understanding of the fundamental interactions essential to replication of this
540 important human pathogen and for future studies towards specific antiviral
541 therapies.
542

543 **Funding**

544 This work was supported by funding from the MRC to AT (MR/NO1054X/1).
545

546 **Data availability statement**

547 The data underlying this article will be shared on reasonable request to the
548 corresponding author.
549

550 **REFERENCES**

551

552 1. Fong, S.W., R.M. Kini, and L.F.P. Ng, *Mosquito Saliva Reshapes Alphavirus*
553 *Infection and Immunopathogenesis.* Journal of Virology, 2018. **92**(12).
554 2. McPherson, R.L., et al., *ADP-ribosylhydrolase activity of Chikungunya virus*
555 *macrodomain is critical for virus replication and virulence.* Proceedings of the
556 National Academy of Sciences of the United States of America, 2017. **114**(7):
557 p. 1666-1671.
558 3. Petitdemange, C., N. Wauquier, and V. Vieillard, *Control of immunopathology*
559 *during chikungunya virus infection.* Journal of Allergy and Clinical

560 Immunology, 2015. **135**(4): p. 846-855.
561 4. Ng, L.F., *Immunopathology of Chikungunya virus infection: lessons learned*
562 *from patients and animal models.* Annual review of virology, 2017. **4**: p. 413-
563 427.
564 5. Meshram, C.D., et al., *Multiple Host Factors Interact with the Hypervariable*
565 *Domain of Chikungunya Virus nsP3 and Determine Viral Replication in Cell-*
566 *Specific Mode.* J Virol, 2018. **92**(16).
567 6. Rupp, J.C., et al., *Alphavirus RNA synthesis and non-structural protein*
568 *functions.* Journal of General Virology, 2015. **96**(9): p. 2483-2500.
569 7. Tuplin, A., *Diverse roles and interactions of RNA structures during the*
570 *replication of positive-stranded RNA viruses of humans and animals.* J Gen
571 Virol, 2015.
572 8. Frolov, I., R. HARDY, and C.M. RICE, *Cis-acting RNA elements at the 5′ end*
573 *of Sindbis virus genome RNA regulate minus-and plus-strand RNA synthesis.*
574 Rna, 2001. **7**(11): p. 1638-1651.
575 9. Kendall, C., et al., *Structural and phenotypic analysis of Chikungunya virus*
576 *RNA replication elements.* Nucleic Acids Res, 2019. **47**(17): p. 9296-9312.
577 10. Troschel, F.M., et al., *Knockdown of Musashi RNA Binding Proteins*
578 *Decreases Radioresistance but Enhances Cell Motility and Invasion in Triple-*
579 *Negative Breast Cancer.* Int J Mol Sci, 2020. **21**(6).
580 11. Sutherland, J.M., et al., *RNA binding proteins in spermatogenesis: an in depth*
581 *focus on the Musashi family.* Asian J Androl, 2015. **17**(4): p. 529-36.
582 12. Horisawa, K., et al., *The Musashi family RNA-binding proteins in stem cells.*
583 Biomol Concepts, 2010. **1**(1): p. 59-66.
584 13. Chavali, P.L., et al., *Neurodevelopmental protein Musashi-1 interacts with the*
585 *Zika genome and promotes viral replication.* Science, 2017. **357**(6346): p. 83-
586 88.
587 14. Tsetsarkin, K., et al., *Infectious clones of Chikungunya virus (La Reunion*
588 *isolate) for vector competence studies.* Vector Borne Zoonotic Dis, 2006. **6**(4):
589 p. 325-37.
590 15. Pohjala, L., et al., *Inhibitors of alphavirus entry and replication identified with*
591 *a stable Chikungunya replicon cell line and virus-based assays.* PloS one,
592 2011. **6**(12): p. e28923.

593 16. Lello, L.S., et al., *Cross-utilisation of template RNAs by alphavirus replicases.*
594 PLoS Pathog, 2020. **16**(9): p. e1008825.
595 17. Muller, M., et al., *Chikungunya virus requires cellular chloride channels for*
596 *efficient genome replication.* PLoS Negl Trop Dis, 2019. **13**(9): p. e0007703.
597 18. Bartholomeeusen, K., et al., *A Chikungunya Virus trans-Replicase System*
598 *Reveals the Importance of Delayed Nonstructural Polyprotein Processing for*
599 *Efficient Replication Complex Formation in Mosquito Cells.* J Virol, 2018.
600 **92**(14).
601 19. Clingman, C.C., et al., *Allosteric inhibition of a stem cell RNA-binding protein*
602 *by an intermediary metabolite.* Elife, 2014. **3**: p. e02848.
603 20. Arkin, M.R. and J.A. Wells, *Small-molecule inhibitors of protein–protein*
604 *interactions: progressing towards the dream.* Nature reviews Drug discovery,
605 2004. **3**(4): p. 301-317.
606 21. Niederhauser, O., et al., *NGF ligand alters NGF signaling via p75NTR and*
607 *TrkA.* Journal of neuroscience research, 2000. **61**(3): p. 263-272.
608 22. Minuesa, G., et al., *Small-molecule targeting of MUSASHI RNA-binding*
609 *activity in acute myeloid leukemia.* Nature communications, 2019. **10**(1): p. 1-
610 15.
611 23. Lello, L.S., et al., *Cross-utilisation of template RNAs by alphavirus replicases.*
612 PLoS pathogens, 2020. **16**(9): p. e1008825.
613 24. Roberts, G.C., et al., *Evaluation of a range of mammalian and mosquito cell*
614 *lines for use in Chikungunya virus research.* Scientific reports, 2017. **7**(1): p.
615 1-13.
616 25. Zearfoss, N.R., et al., *A conserved three-nucleotide core motif defines Musashi*
617 *RNA binding specificity.* J Biol Chem, 2014. **289**(51): p. 35530-41.
618 26. Matkovic, R., et al., *The Host DHX9 DExH-Box Helicase Is Recruited to*
619 *Chikungunya Virus Replication Complexes for Optimal Genomic RNA*
620 *Translation.* Journal of Virology, 2019. **93**(4).
621
622 **Figure Legends:**
623
624 **Figure 1. A)** Schematic representation of CHIKV genome organisation **B)** Schematic
625 representation of CHIKV RNA structures within the 5'UTR and adjacent ORF-1 region

626 of the CHIKV genome (Kendall et al., 2019). RNA replication elements SL3, SL47,
627 SL88, SL102, SL165, SL194 and SL246 are labelled in black type. The ORF-1 AUG start
628 codon is labelled by a green arrow and the putative MSI binding site by a red oval.
629
630 **Figure 2.** Ro signifyingly inhibits replication of infectious CHIKV and the CHIKV-SGR **A)**
631 Schematic representations of CHIKV infectious clone (top) compared to the sub-
632 genomic replicon (SGR) (bottom) in which a *Renilla* luciferase (RLuc) reporter gene is
633 fused within the nsp3 coding sequence and the structural genes of ORF-2 are
634 replaced by a firefly luciferase (Fluc) reporter gene. Replication is expressed in
635 Relative Light Units [RLU] **B)** Ro significantly inhibits productive CHIKV productive
636 replication relative to DMSO treated negative controls at 8 and 24 hpi. **C** and **D)** Ro
637 08-2750 significantly inhibits CHIKV-SGR replication, measured by both ORF-1 and
638 ORF-2 expression, relative to DMSO treated negative controls at 8 and 24 hpt. N=3,
639 error bars represent standard error from the mean and significance was measured
640 by two-tailed T-test (* = P < 0.05, ** = P < 0.01, *** = P < 0.001).
641
642 **Figure 3.** Ro signifyingly inhibits CHIKV genome replication. **A)** Schematic
643 representation of CHIKV *trans*-complementation assay showing codon optimised
644 pCHIKV-nsP1234 (top) from which the CHIKV nsPs were translated and pCHIK-
645 Fluc/Gluc (bottom) in which ORF-1 was replaced by an Fluc reporter gene, fused to
646 the first 77 nts or CHIKV ORF-1 (N77) down-stream of the authentic CHIKV 5'UTR.
647 ORF-2, flanked by the authentic intragenic (SG) and 3' UTRs, was replaced by a Gluc
648 reporter gene. **B** and **C)** Ro significantly inhibited CHIKV genome replication of the
649 *trans*-complementation assay, measured by both ORF-1 and ORF-2 expression,
650 relative to DMSO treated negative controls at 8 and 24 hpt. N=3, error bars
651 represent standard error from the mean and significance was measured by two-
652 tailed T-test (* = P < 0.05, ** = P < 0.01, *** = P < 0.001).
653
654 **Figure 4.** shRNA suppression of MSI-2 significantly inhibits replication of infectious
655 CHIKV. **A)** Western blot analysis of total cellular protein extracted from Rd cells and
656 compared to negative control scrambled shRNA, demonstrated consistent shRNA

657 knockdown of MSI-2 over 3 serial passages (P1- P3). MSI-2 suppression significantly
658 inhibited productive CHIKV replication, relative to scrambled shRNA at 8 and 24 hpi
659 measured by plaque assay **B)** and strand specific qRT-PCR for the the virus genomic
660 **C)** and negative intermediate **D)** strands. N=3, error bars represent standard error
661 from the mean and significance was measured by two-tailed T-test (* = P < 0.05, ** =
662 P < 0.01, *** = P < 0.001).
663
664 **Figure 5.** shRNA suppression of MSI-2 significantly inhibits CHIKV-SGR replication and
665 CHIKV genome replication. **A** and **B)** shRNA suppression of MSI-2 significantly
666 inhibited CHIKV-SGR replication, measured by both ORF-1 and ORF-2 expression,
667 relative to scrambled shRNA negative controls at 8 and 24 hpt. **C** and **D)** shRNA
668 suppression of MSI-2 significantly inhibited CHIKV genome replication of the *trans*-
669 complementation assay, measured by both ORF-1 and ORF-2 expression, relative to
670 DMSO treated negative controls at 8 and 24 hpt. N=3, error bars represent standard
671 error from the mean and significance was measured by two-tailed T-test (* = P <
672 0.05, ** = P < 0.01, *** = P < 0.001).
673
674 **Figure 6**. siRNA Depletion of either MSI-1 or MSI-2 significantly inhibited CHIKV
675 replication in Huh7 cells and co-depletion of both MSI-1 and MSI-2 had a synergistic
676 effect on CHIKV inhibition in Huh7 cells. siRNA depletion of MSI-2 significantly
677 inhibited CHIKV replication in RD cells and co-depletion of both MSI-1 and MSI-2 did
678 not increase the level of CHIKV inhibition. siRNA depletion of MSI-1 and MSI-2
679 significantly inhibited CHIKV replication in Huh7 cells relative to scrambled siRNA at 8
680 and 24 hpi measured by plaque assay **A)** and strand specific qRT-PCR for the the virus
681 genomic **B)** and negative intermediate **C)** strands. siRNA depletion of MSI-2 in RD
682 cells significantly inhibited CHIKV replication in relative to scrambled siRNA at 8 and
683 24 hpi measured by plaque assay **D)** and strand specific qRT-PCR for the the virus
684 genomic **E)** and negative intermediate **F)** strands. N=3, error bars represent standard
685 error from the mean and significance was measured by two-tailed T-test (* = P <
686 0.05, ** = P < 0.01, *** = P < 0.001).
687

688 **Figure 7.** Native EMSAs between *in vitro* transcribed ^{32}P 5' radiolabeled CHIKV RNA
689 nts 1-330 (*RNA^{WT}) and recombinantly expressed MSI-2 demonstrated an
690 RNA/protein interaction that was outcompeted by increasing concentrations of
691 equivalent unlabeled (RNA^{WT}) but less efficiently by the same RNA incorporating
692 BSM mutation $_{63}$AUUAAU$_{68}$ >$_{63}$CAACUU$_{68}$ (RNA^{BSM}). **A)** Increasing concentrations of
693 MSI-2 intensified the observed band shift to the larger RNA/Protein complex and
694 decreased the equivalent unbound RNA band. The interaction between a 1:4 ratio of
695 *RNA^{WT}:MSI-2 was competed with increasing concentrations of unlabelled **B)** RNA^{WT}
696 or **C)** RNA^{mut} ($_{63}$CAACUU$_{68}$-mut). **D)** Band shifts in the unlabeled RNA competition
697 EMSAs were quantified by densitometry and expressed as % change in the density of
698 the RNA/Protein complex bands, normalized to the equivalent total lane density, for
699 each competition ratio and compared each time to ratio 1:0. N=3, error bars
700 represent standard error from the mean and significance was measured by two-
701 tailed T-test (* = P < 0.05, ** = P < 0.01, *** = P < 0.001). Grey block triangles
702 indicate increasing concentrations of specific reactants.
703
704 **Figure 8.** Substitutions within the predicted MSI binding site ($_{63}$CAACUU$_{68}$-mut)
705 prevented rescue of BSM-mutant virus and significantly inhibited CHIKV genome
706 replication. **A** and **B)** Mutation of the MSI binding site significantly inhibited CHIKV
707 genome replication of the *trans*-complementation assay, measured by both ORF-1
708 and ORF-2 expression, relative to wild-type positive controls at 8 and 24 hpt. **C)**
709 Mutation of the predicted MSI binding site prevented rescue of BSM-mutant CHIKV
710 following transfection of capped *in vitro* transcribed RNA into BHK cells. Released
711 virus was measured by plaque assay of supernatant 24 hpt and compared to positive
712 control wild-type infectious CHIKV *in vitro* transcribed RNA, which was transfected
713 and analysed in parallel. N=3, error bars represent standard error from the mean and
714 significance was measured by two-tailed T-test (* = P < 0.05, ** = P < 0.01, *** = P <
715 0.001).

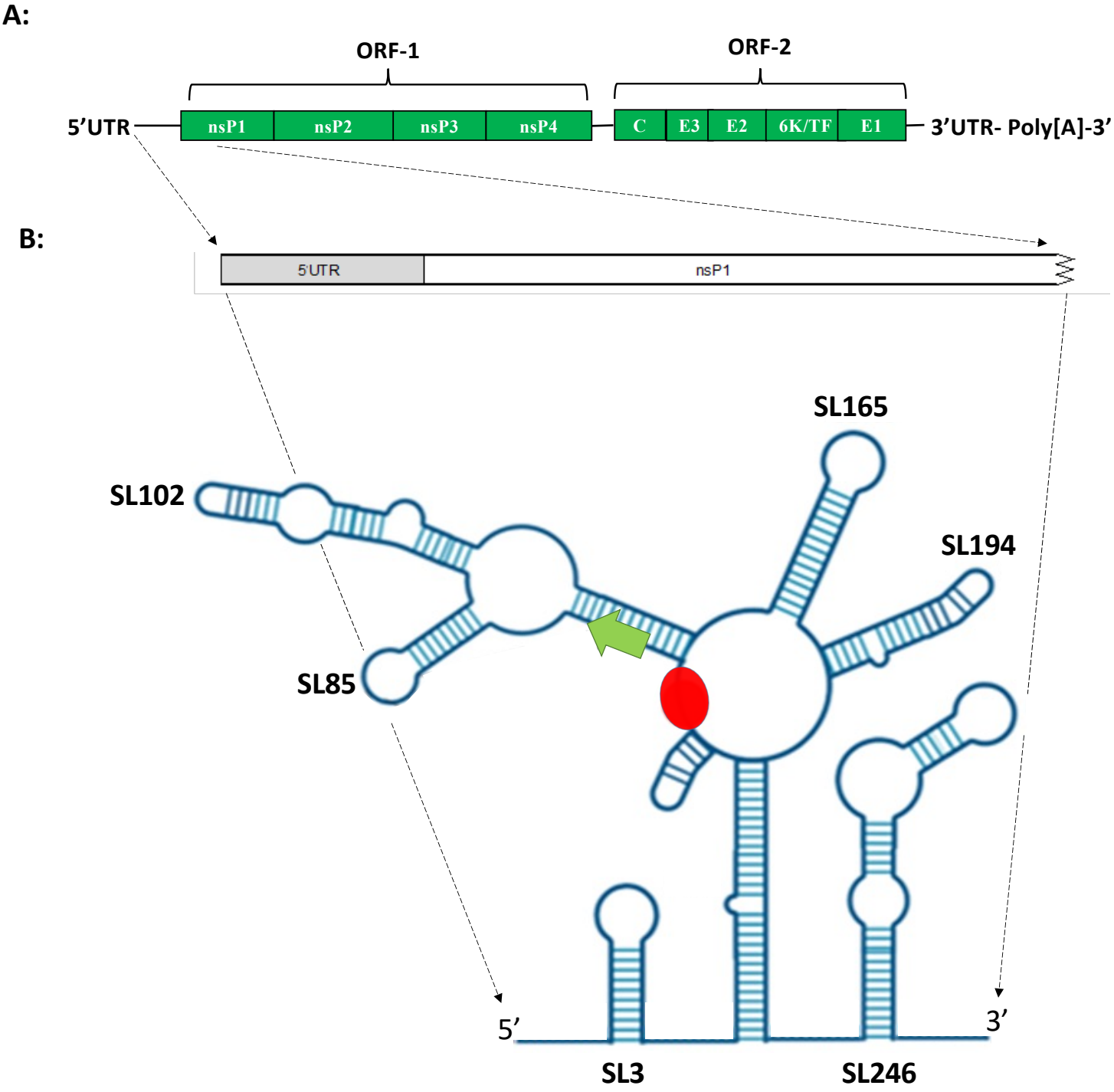

Figure 1. A) Schematic representation of CHIKV genome organisation **B)** Schematic representation of CHIKV RNA structures within the 5'UTR and adjacent ORF-1 region of the CHIKV genome (Kendall et al., 2019). RNA replication elements SL3, SL47, SL88, SL102, SL165, SL194 and SL246 are labelled in black type. The ORF-1 AUG start codon is labelled by a green arrow and the putative MSI binding site by a red oval

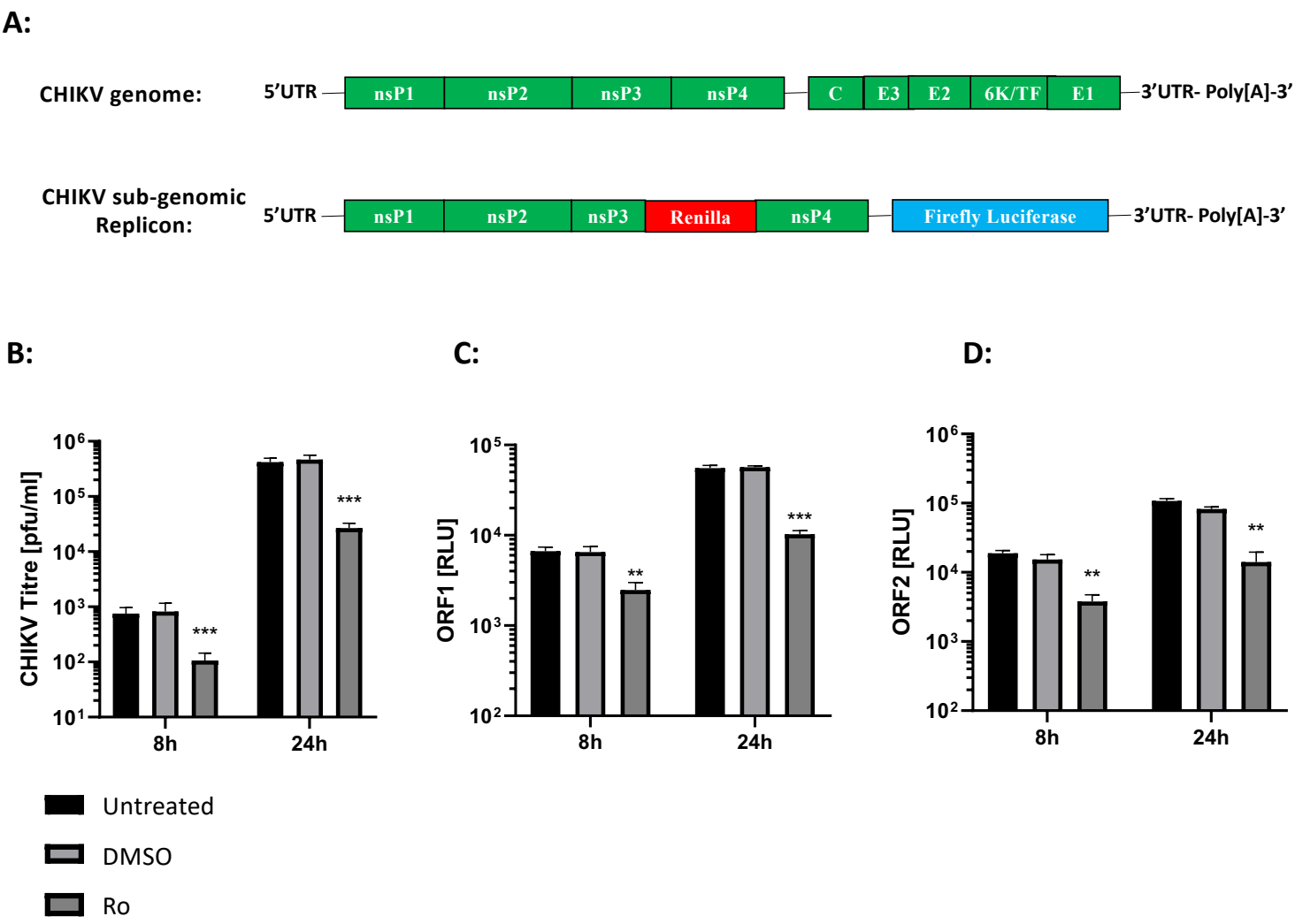

Figure 2. Ro signifyingly inhibits replication of infectious CHIKV and the CHIKV-SGR A) Schematic representations of CHIKV infectious clone (top) compared to the sub-genomic replicon (SGR) (bottom) in which a *Renilla* luciferase (RLuc) reporter gene is fused within the nsp3 coding sequence and the structural genes of ORF-2 are replaced by a firefly luciferase (Fluc) reporter gene. Replication is expressed in Relative Light Units [RLU] **B)** Ro significantly inhibits productive CHIKV productive replication relative to DMSO treated negative controls at 8 and 24 hpi. **C and D)** Ro 08-2750 significantly inhibits CHIKV-SGR replication, measured by both ORF-1 and ORF-2 expression, relative to DMSO treated negative controls at 8 and 24 hpt. N=3, error bars represent standard error from the mean and significance was measured by two-tailed T-test (* = P < 0.05, ** = P < 0.01, *** = P < 0.001).

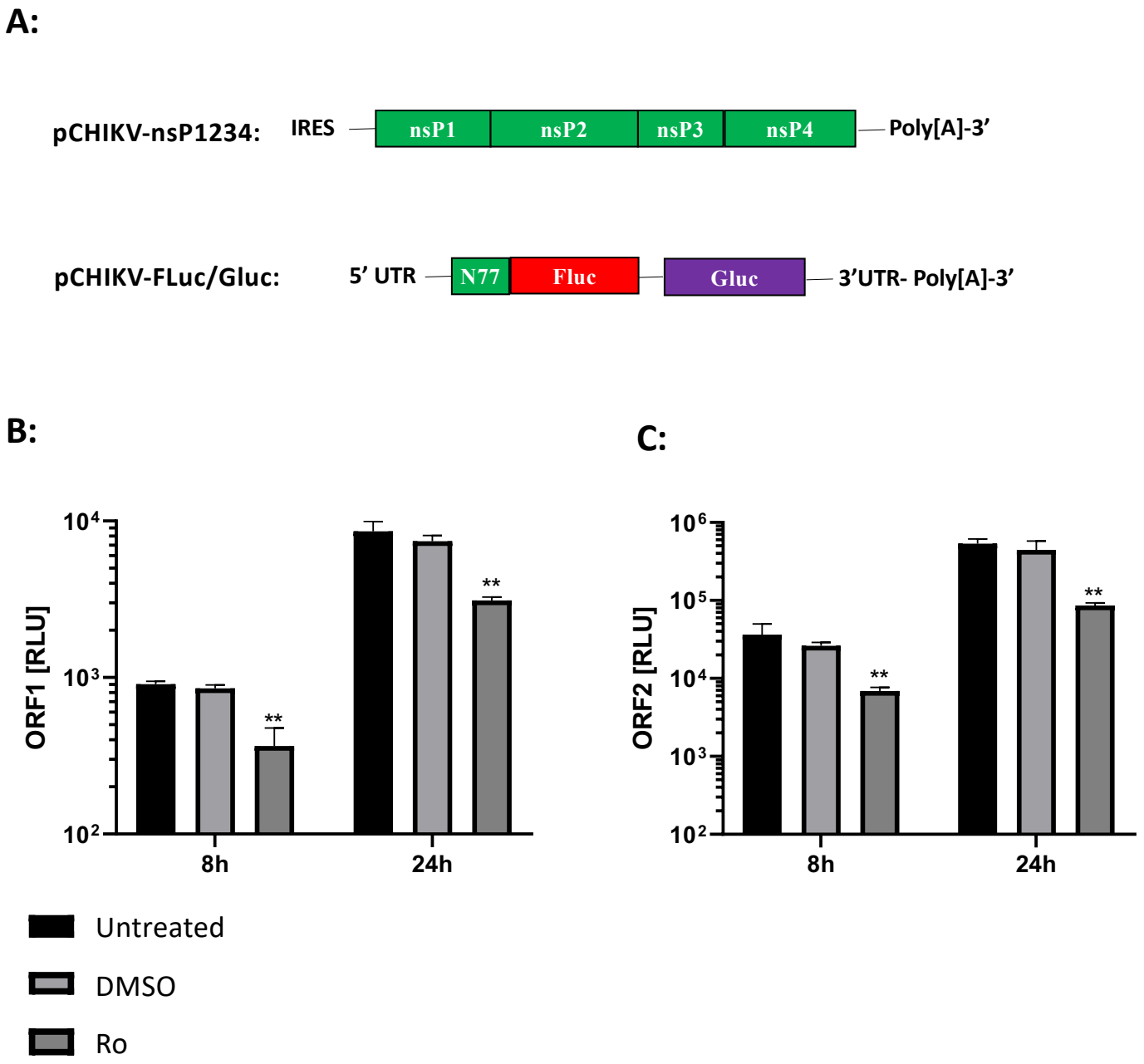

Figure 3. Ro signifyingly inhibits CHIKV genome replication. A) Schematic representation of CHIKV *trans*-complementation assay showing codon optimised pCHIKV-nsP1234 (top) from which the CHIKV nsPs were translated and pCHIK-Fluc/Gluc (bottom) in which ORF-1 was replaced by an Fluc reporter gene, fused to the first 77 nts or CHIKV ORF-1 (N77) down stream of the authentic CHIKV 5'UTR. ORF-2, flanked by the authentic intragenic (SG) and 3' UTRs, was replaced by a Gluc reporter gene. **B and C)** Ro significantly inhibited CHIKV genome replication of the *trans*-complementation assay, measured by both ORF-1 and ORF-2 expression, relative to DMSO treated negative controls at 8 and 24 hpt. N=3, error bars represent standard error from the mean and significance was measured by two-tailed T-test (* = $P < 0.05$, ** = $P < 0.01$, *** = $P < 0.001$).

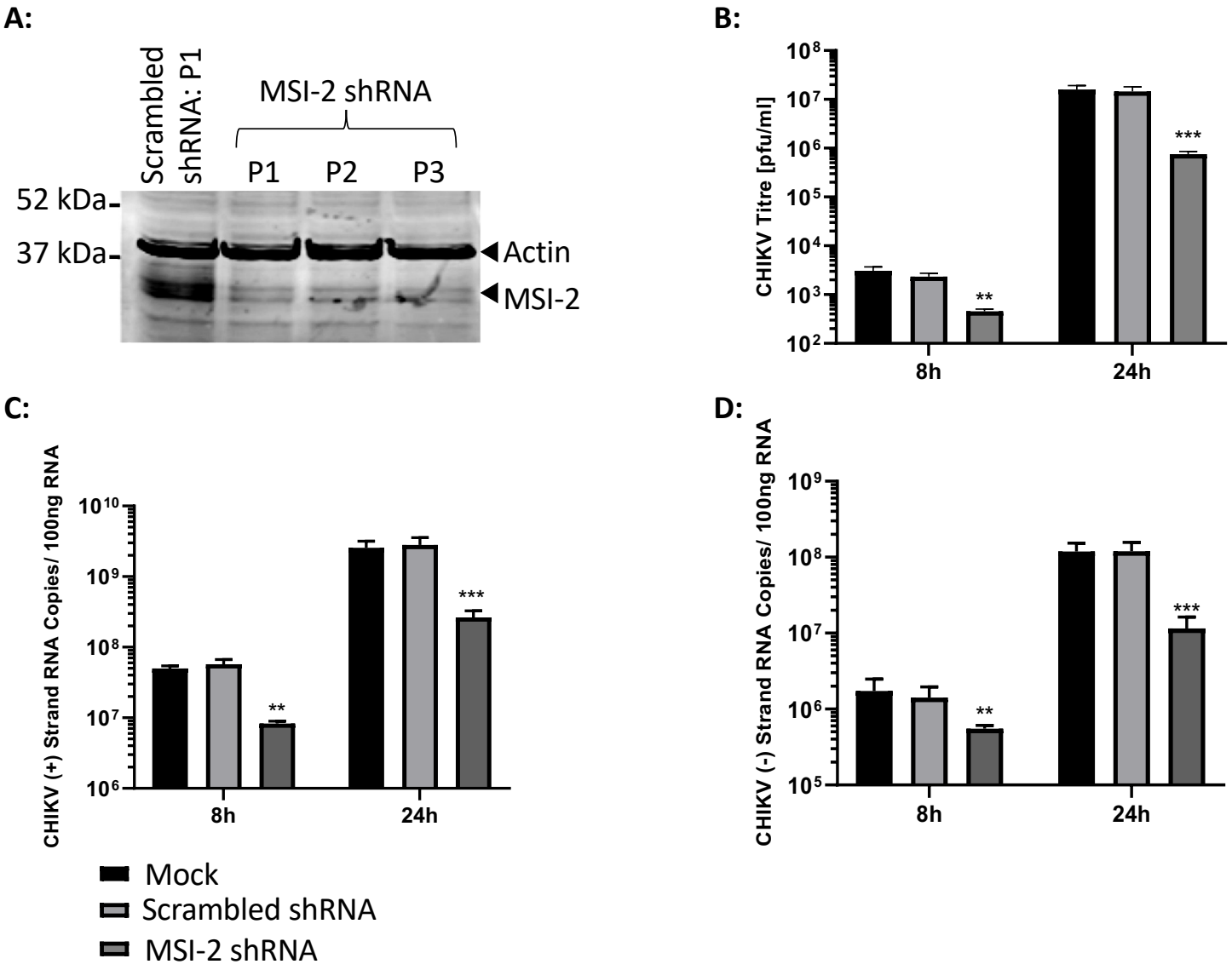

Figure 4. shRNA suppression of MSI-2 significantly inhibits replication of infectious CHIKV. A) Western blot analysis of total cellular protein extracted from Rd cells and compared to negative control scrambled shRNA, demonstrated consistent shRNA knockdown of MSI-2 over 3 serial passages (P1- P3). MSI-2 suppression significantly inhibited productive CHIKV replication, relative to scrambled shRNA at 8 and 24 hpi measured by plaque assay **(B)** and strand specific qRT-PCR for the the virus genomic **(C)** and negative intermediate **(D)** strands. N=3, error bars represent standard error from the mean and significance was measured by two-tailed T-test (* = P < 0.05, ** = P < 0.01, *** = P < 0.001).

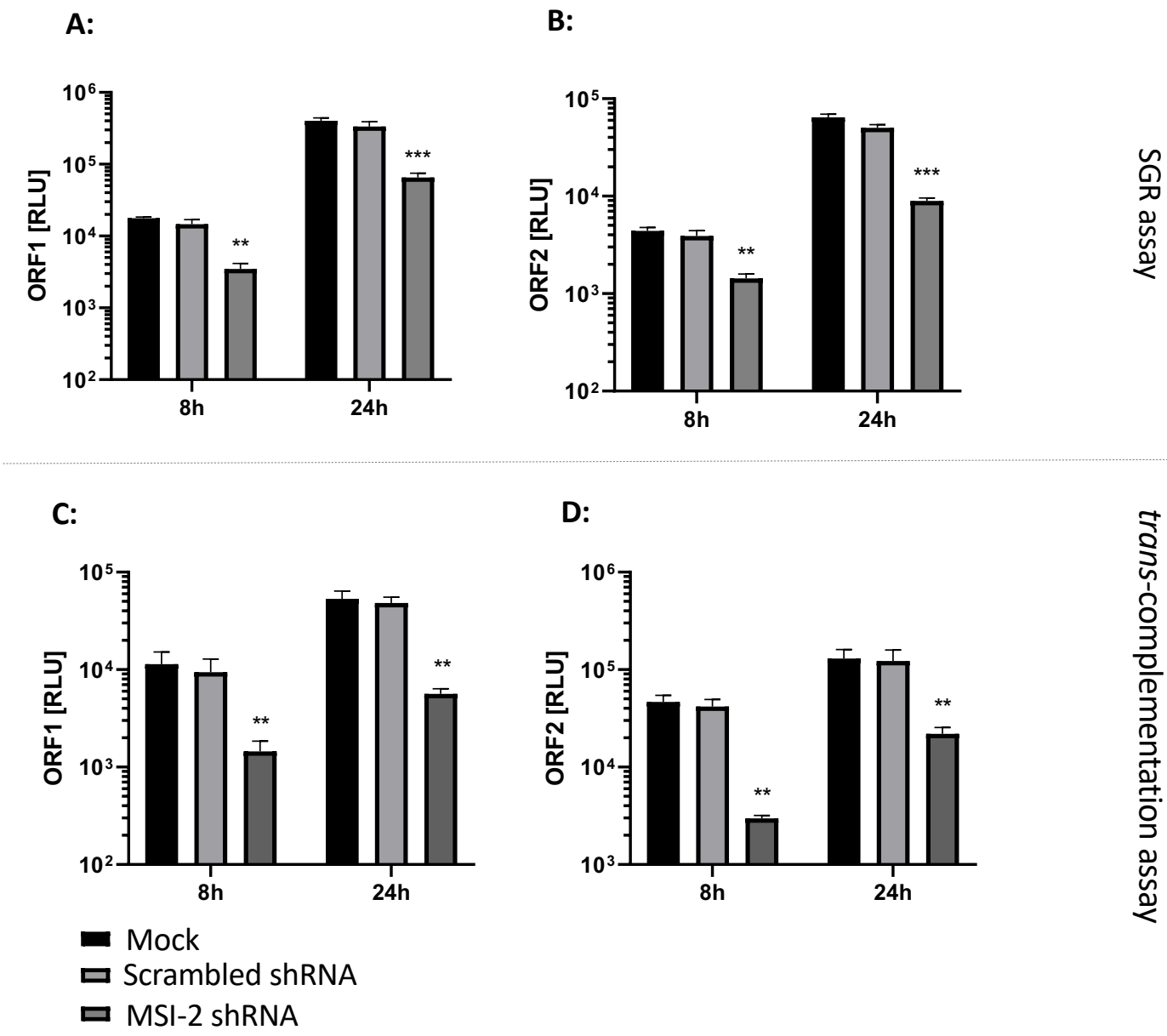

Figure 5. shRNA suppression of MSI-2 significantly inhibits CHIKV-SGR replication and CHIKV genome replication. A and **B)** shRNA suppression of MSI-2 significantly inhibited CHIKV-SGR replication, measured by both ORF-1 and ORF-2 expression, relative to scrambled shRNA negative controls at 8 and 24 hpt. **C** and **D**) shRNA suppression of MSI-2 significantly inhibited CHIKV genome replication of the *trans*-complementation assay, measured by both ORF-1 and ORF-2 expression, relative to DMSO treated negative controls at 8 and 24 hpt. N=3, error bars represent standard error from the mean and significance was measured by two-tailed T-test (* = P < 0.05, ** = P < 0.01, *** = P < 0.001).

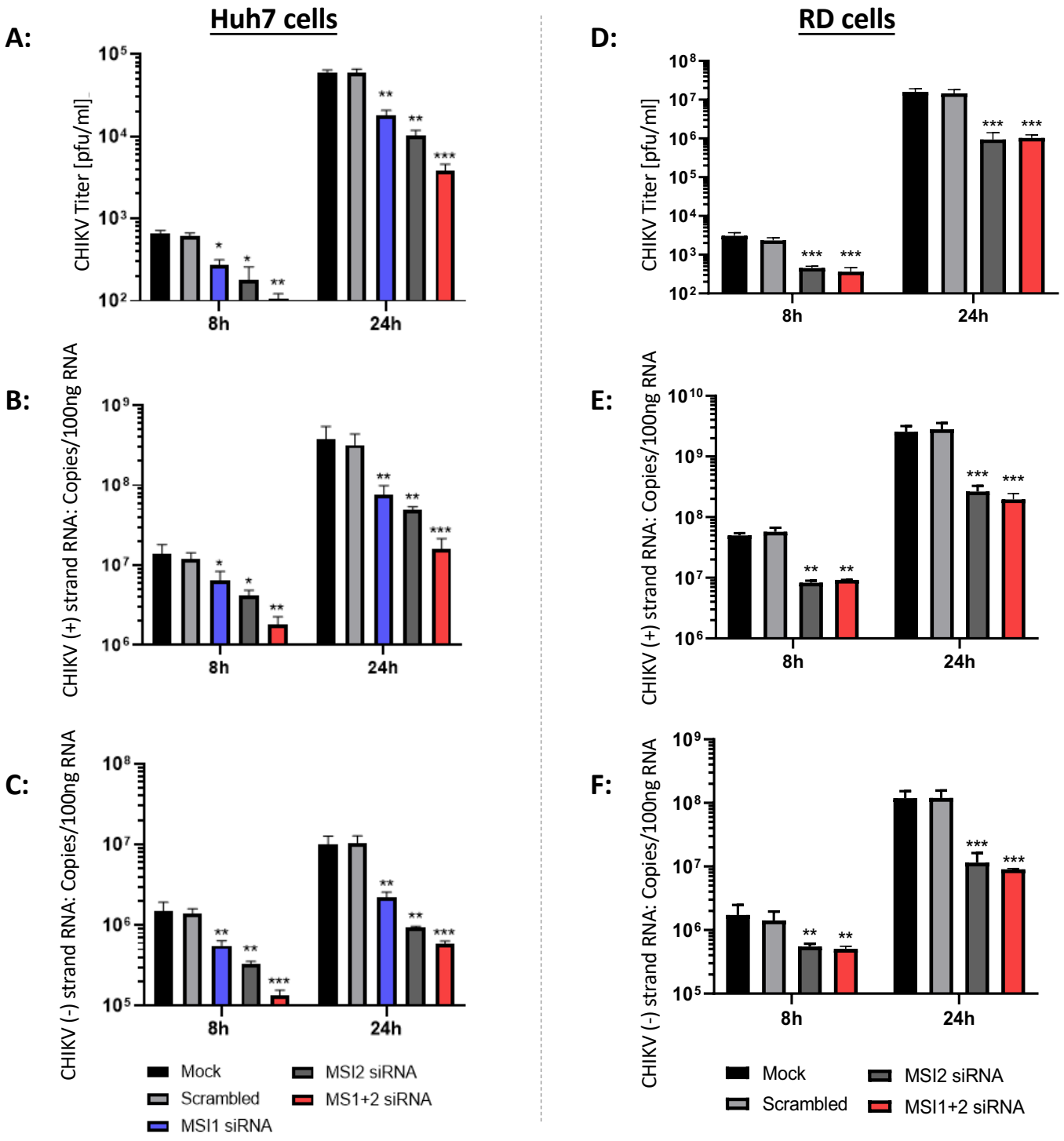

Figure 6: siRNA Depletion of either MSI-1 or MSI-2 significantly inhibited CHIKV replication in Huh7 cells and co-depletion of both MSI-1 and MSI-2 had a synergistic affect on CHIKV inhibition in Huh7 cells. siRNA depletion of MSI-2 significantly inhibited CHIKV replication in RD cells and co-depletion of both MSI-1 and MSI-2 did not increase the level of CHIKV inhibition. siRNA depletion of MSI-1 and MSI-2 significantly inhibited CHIKV replication in Huh7 cells relative to scrambled siRNA at 8 and 24 hpi measured by plaque assay **(A)** and strand specific qRT-PCR for the the virus genomic **(B)** and negative intermediate **(C)** strands. siRNA depletion of MSI-2 in RD cells significantly inhibited CHIKV replication in relative to scrambled siRNA at 8 and 24 hpi measured by plaque assay **(D)** and strand specific qRT-PCR for the the virus genomic **(E)** and negative intermediate **(F)** strands. N=3, error bars represent standard error from the mean and significance was measured by two-tailed T-test (* = $P < 0.05$, ** = $P < 0.01$, *** = $P < 0.001$).

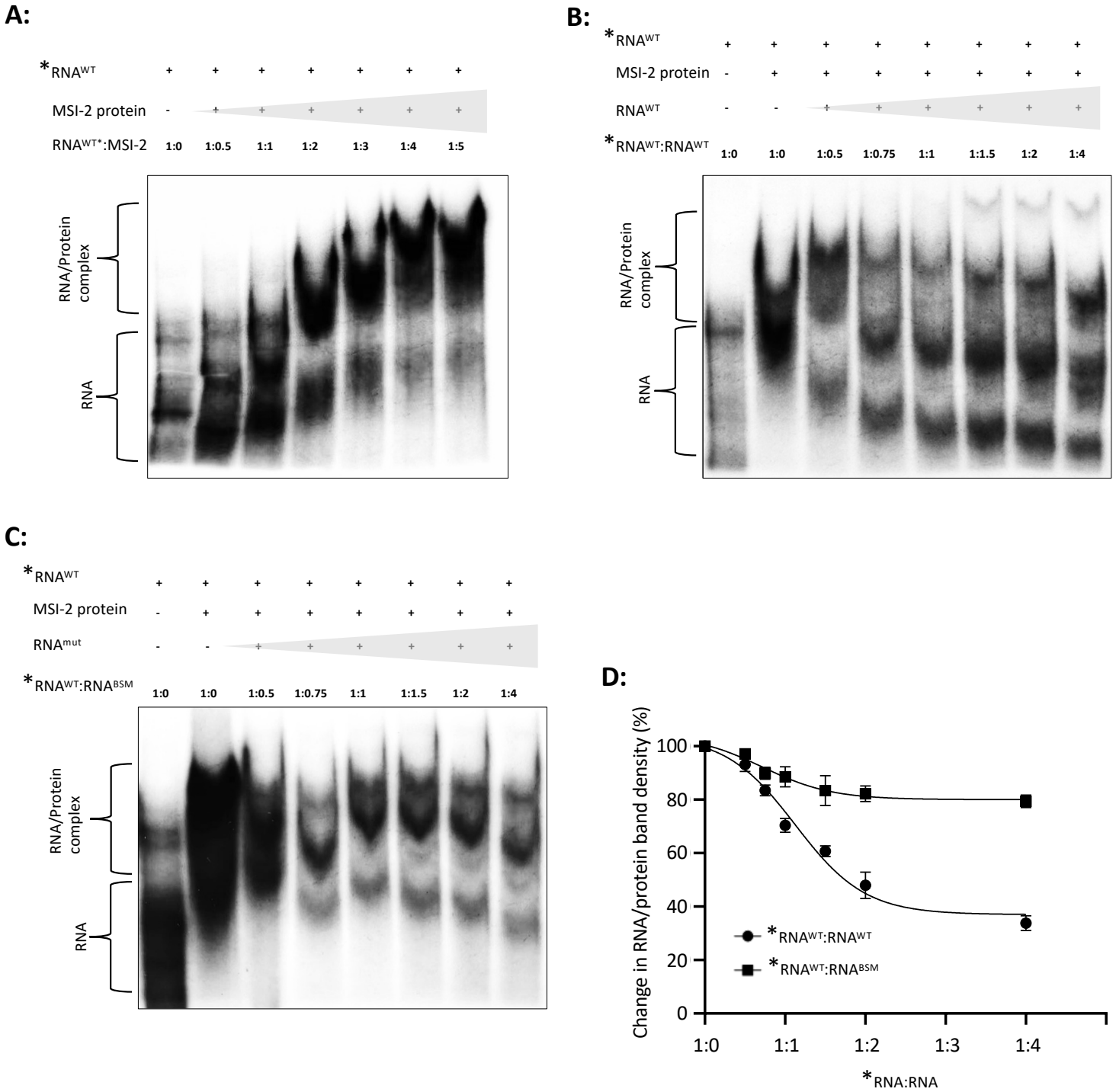

Figure 7. Native EMSAs between *in vitro* transcribed P^{32} 5' radiolabeled CHIKV RNA nts 1-330 (*RNA^{WT}) and recombinantly expressed MSI-2 demonstrated an RNA/protein interaction that was outcompeted by increasing concentrations of equivalent unlabeled (RNA^{WT}) but less efficiently by the same RNA incorporating BSM mutation $_{63}AUUAAU_{68}$ >$_{63}CAACUU_{68}$ (RNA^{BSM}). A) Increasing concentrations of MSI-2 intensified the observed band shift to the larger RNA/Protein complex and decreased the equivalent unbound RNA band. The interaction between a 1:4 ratio of *RNA^{WT}:MSI-2 was competed with increasing concentrations of unlabelled **B)** RNA^{WT} or **C)** RNA^{mut} ($_{63}CAACUU_{68}$-mut). **D)** Band shifts in the unlabeled RNA competition EMSAs were quantified by densitometry and expressed as % change in the density of the RNA/Protein complex bands, normalized to the equivalent total lane density, for each competition ratio and compared each time to ratio 1:0. N=3, error bars represent standard error from the mean and significance was measured by two-tailed T-test (* = P < 0.05, ** = P < 0.01, *** = P < 0.001). Grey block triangles indicate increasing concentrations of specific reactants.

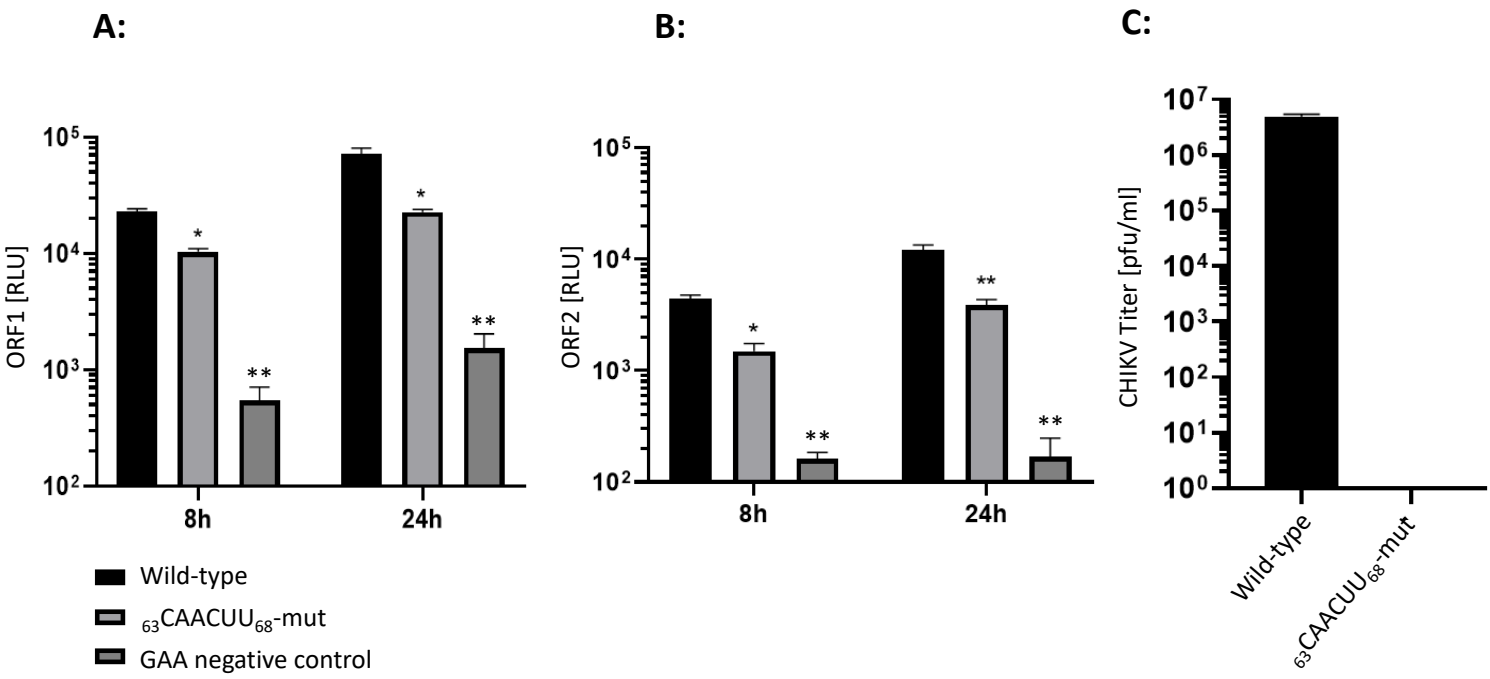

Figure 8. Substitutions within the predicted MSI binding site ($_{63}$CAACUU$_{68}$-mut) prevented rescue of BSM-mutant virus and significantly inhibited CHIKV genome replication. **A and B)** Mutation of the MSI binding site significantly inhibited CHIKV genome replication of the *trans*-complementation assay, measured by both ORF-1 and ORF-2 expression, relative to wild-type positive controls at 8 and 24 hpt. **C)** Mutation of the predicted MSI binding site prevented rescue of BSM-mutant CHIKV following transfection of capped *in vitro* transcribed RNA into BHK cells. Released virus was measured by plaque assay of supernatant 24 hpt and compared to positive control wild-type infectious CHIKV *in vitro* transcribed RNA, which was transfected and analysed in parallel. N=3, error bars represent standard error from the mean and significance was measured by two-tailed T-test (* = P < 0.05, ** = P < 0.01, *** = P < 0.001).

Supplementary data 1: Primers for the reverse transcription and quantitative PCRs for CHIKV strand-specific detection.

CIKV (-) strand detection	PCR	Primer sequence (5'-3')
CHIKV FT tag T	reverse transcription	GGC AGT ATC GTG AAT TCG ATG CGA CAC GGA GAC GCC AAC ATT
Tag T	quantitative	GGC AGT ATC GTG AAT TCG ATG C
CHIKV R T	quantitative	AAT AAA TCA TAA GTC TGC TCT CTG TCT ACA TGA
CHIKV (+) strand detection	PCR	Primer sequence (5'-3')
CHIKV RT tag T	reverse transcription	GGC AGT ATC GTG AAT TCG ATG CGT CTG CTC TCT GTC TAC ATG A
CHIKV F T	quantitative	AAT AAA TCA TAA GAC ACG GAG ACG CCA ACA TT
Tag T	quantitative	see above

Supplementary data 2: Expression and purification of MSI-2 Coomassie stained PAGE analysis following **A)** His Tag and **B)** Ion exchange chromatography. **C)** Ion exchange purified MSI-2 (8-193) analyzed by western blot, relative to total protein extracted from RD and Huh7 cells.

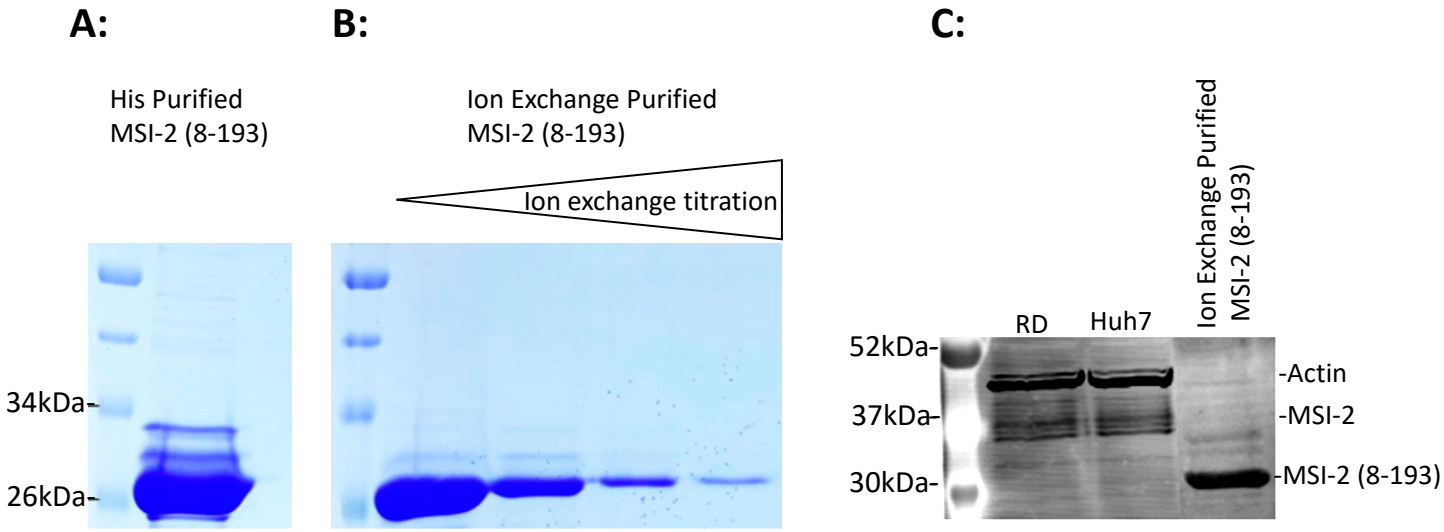

Supplementary data 3: MTT cytotoxicity assay for Ro 08-2750 in RD cells across a titration of 0, 05, 1, 3, 5 10 and 20uM. N=3, error bars represent standard error from the mean.

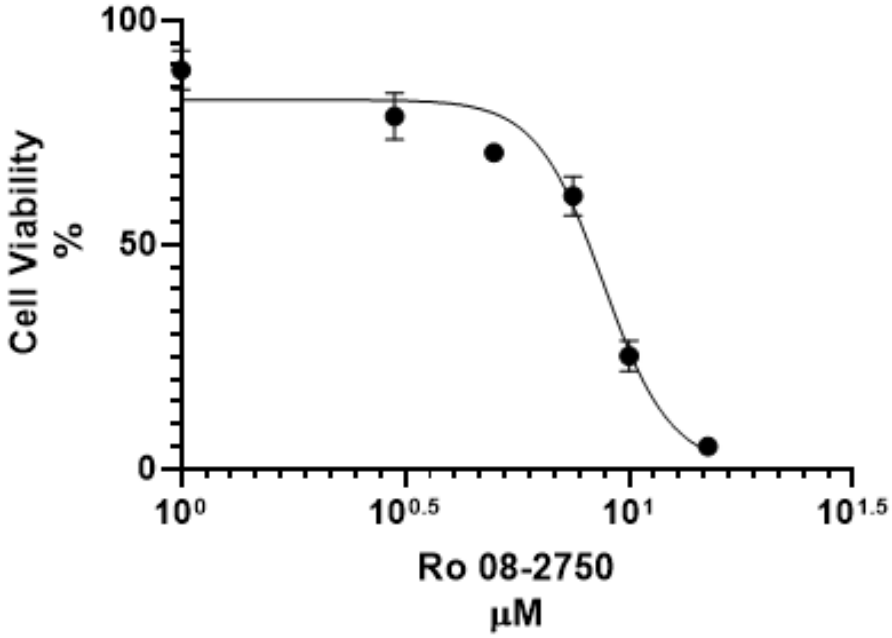

Supplementary data 4: A) MSI-1 and **B**) MSI-2 expression in RD and Huh7 cell lysate analyzed by western blot.

A)

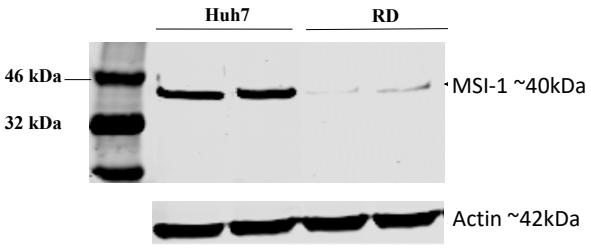

B)

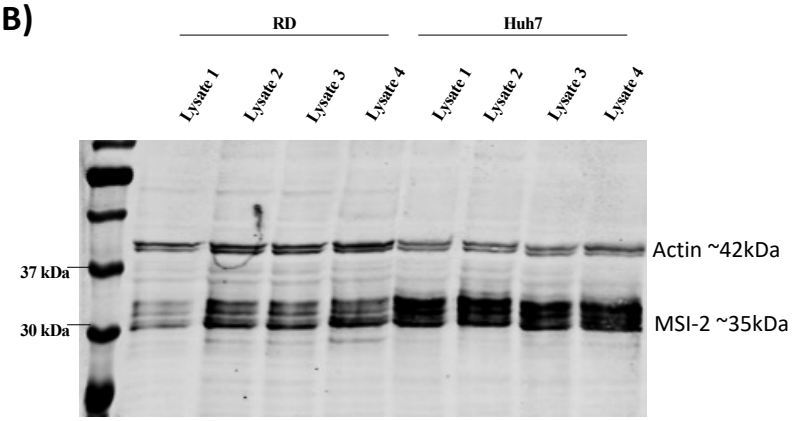
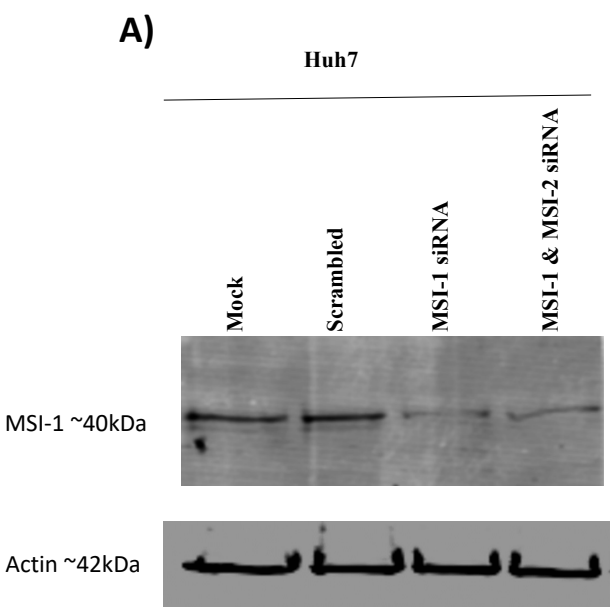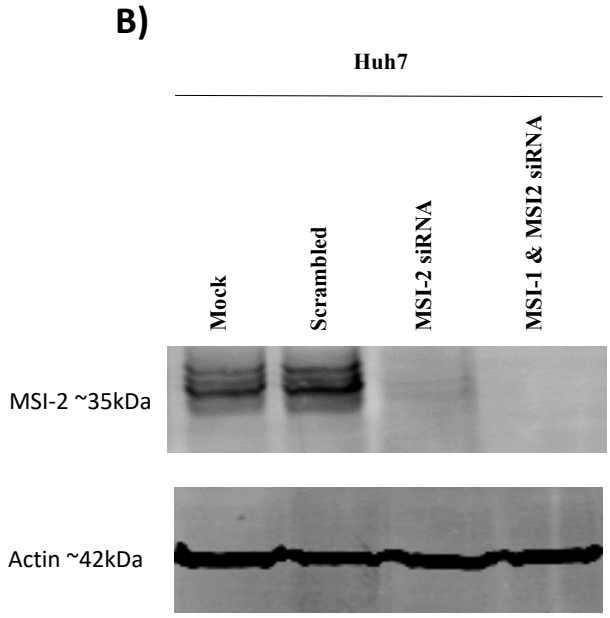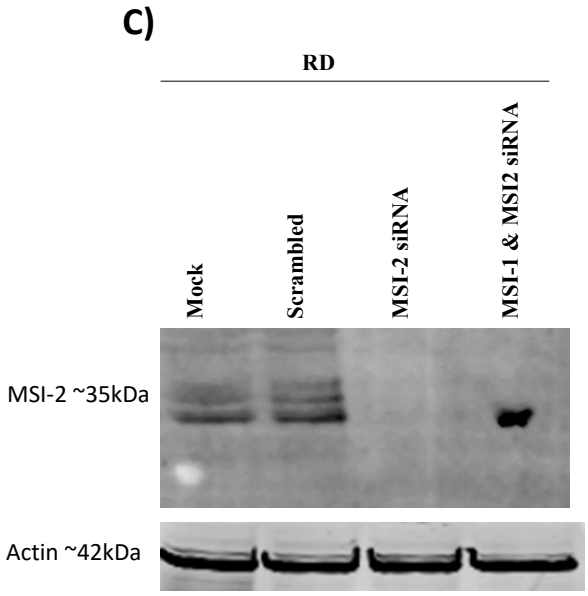
Supplementary data 5: Co-inhibition of MSI-2 and MSI-1 by siRNA in **A)** and **B)** Huh7 cells and **C)** RD cells